

Dynamical effects on vibrational and electronic spectra of hydroperoxyl radical water clusters

Srinivasan S. Iyengar^{a)}

Department of Chemistry and Department of Physics, Indiana University, 800 E. Kirkwood Avenue, Bloomington, Indiana 47405

(Received 17 May 2005; accepted 30 June 2005; published online 29 August 2005)

We have carried out *ab initio* molecular-dynamics studies on hydroperoxyl water clusters. Our studies are complemented by optimization, frequency, and excited-state calculations. The three main results we obtained are (a) the dynamically averaged energy gap between the highest-occupied molecular orbital and the lowest-unoccupied molecular orbital monotonically decreases as the number of water molecules is increased in a hydroperoxyl water cluster system, (b) the dynamical averaging of the potential-energy surface at finite temperature broadens the electronic excitation spectrum and changes the infrared spectrum in nontrivial ways, and (c) the structural analysis of our dynamics simulation indicates that the oxygen-oxygen distance in a solvated hydroperoxyl-water cluster is very similar to that found in protonated water clusters (Zundel: H_5O_2^+) in spite of the fact that the latter possesses a positive charge and the hydroperoxyl-water cluster does not. Dynamical charge analysis and the weak acidity of HO_2 are used to justify this result. © 2005 American Institute of Physics. [DOI: 10.1063/1.2006674]

I. INTRODUCTION

Water clusters provide sites for heterogeneous chemical reactions in the earth's atmosphere.¹⁻¹² Thus medium-sized water clusters have been used to model cloud droplets¹³ and aerosols¹⁴ in atmospheric science. Numerous molecules are known to solvate in such water clusters. This has led to several studies analyzing the stability of HCl ,^{3,15,16} H_2SO_4 ,¹⁷ N_2O_5 , ClONO_2 ,¹⁷ HO_2 ,^{5,6,13,18-21} and ions such as H_3O^+ ,²²⁻⁵⁰ OH^- ,⁵¹⁻⁵³ halides,⁵⁴⁻⁵⁷ and metal ions^{58,59} in water clusters. Understanding the stability, dynamics, and mechanism of incorporation of ionic solutes and free radicals constitutes an important challenge to both theory and experiment. The challenge to theory arises from the fact that weak intermolecular interactions, polarizability of water,⁶⁰ and the rapid change in topography of the potential-energy surface at finite temperature dominate important structural and spectroscopic properties in water-clusters.^{25,27}

The behavior of gas-phase radicals, such as the hydroperoxyl radical (HO_2), in water clusters is important in atmospheric science. The hydroperoxyl radical is a major species in the HO_X chemical family² that affects the budgeting of many chemical systems in the atmosphere. The HO_X system plays a central role (along with the OH radical) in oxidative chemistry in the troposphere and ultimately controls the production rate of tropospheric ozone.^{7,13} It is hence considered significant in atmospheric^{2,5} and combustion chemistry.⁶¹ Recent theoretical studies^{13,18} have indicated the HO_2 radical to possess stable interactions with water clusters. Such stability provides an important sink for HO_X systems^{13,14,18,62} in the troposphere. As a result, the structural and dynamical features of water clusters play a vital role in HO_2 -related chemistry.

It was recently found¹³ that a HO_2 molecule preferred to bind to the surface of a 20-water cluster. Similar results have been found for the protonated species in water clusters.²⁵⁻²⁷ However, for the case of HO_2 , the preference for surface only differed from that to the interior by ≈ 1.7 kcal/mol. It has also been noted¹³ that due to this small difference in binding energy, important HO_2 -based chemistry could occur both in the interior as well as on the surface of water clusters at normal atmospheric temperatures. Natural bond orbital analysis of these clusters¹⁸ has revealed the orbital interactions that play a significant role to stabilize the $\text{HO}_2\text{-H}_2\text{O}$ complex. While a critical portion of the stability seems to be due to interactions between an antibonding σ orbital in HO_2 and a bonding σ orbital on a neighboring water, a secondary interaction includes a *back donation* from a nonbonded orbital in HO_2 to an antibonding σ orbital in another neighboring water molecule allowing a stable $\text{HO}_2(\text{H}_2\text{O})_2$ complex to form.

Intrigued by the very minor difference in energy between the "interior" and "surface" configurations of HO_2 as found in Ref. 13, in the current paper we have carried out an *ab initio* molecular dynamical (AIMD)⁶³⁻⁷¹ study of the $\text{HO}_2(\text{H}_2\text{O})_{20}$ cluster at temperatures of atmospheric significance. AIMD constitutes a broad range of methods that allow simultaneous dynamical evolution of nuclei and electrons.^{63-69,71} Although "on-the-fly" approaches to electron-nuclear dynamics are nearly as old as quantum mechanics itself (see, for example, Refs. 72 and 73 for a description of the Dirac-Frenkel time-dependent variational principle, which constitutes a formally exact on-the-fly dynamics scheme) they have generally become indispensable in recent times, on account of efficient computational algorithms^{65,67,68,70,71,74} and faster computational power. Generally, in AIMD, an approximation to the electronic wave

^{a)}Electronic mail: iyengar@indiana.edu

function is propagated along with the nuclear degrees of freedom to simulate dynamics on the Born-Oppenheimer surface. The flavor of AIMD that we use in this paper is called atom-centered density-matrix propagation (ADMP).^{71,74–81} Using ADMP we study the dynamical, temperature, and electronic effects involved in the interaction of HO₂ with a cluster of water molecules. Particularly, we aim to address the issue of stability of the configurations comprising the HO₂ molecule on the interior of the water cluster in the picosecond time scale. We also conduct vibrational and excited-state spectral studies that allow us to comment on the effect of temperature and dynamics on the average structure, reactivity (through its effect on excitation spectra), and infrared spectra of such systems. The dynamical calculations are analyzed for structure using distribution functions and the theoretical spectra are obtained both by computing various time-correlation functions and by carrying out single-point optimization and frequency calculations. Quantum nuclear effects are included within the harmonic approximation,^{82–84} and thermal broadening of excited-state spectrum is also studied.

This paper is organized as follows: In Sec. II we briefly outline ADMP.^{71,74–80} In Sec. III we discuss our results from *ab initio* dynamics and *ab initio* electronic structure calculations of ground- and excited-state properties of HO₂ water clusters. The conclusions are presented in Sec. IV.

II. COMPUTATIONAL METHODOLOGY

In ADMP, the electronic structure is represented using the single-particle density matrix and propagated simultaneously with the classical nuclei through the introduction of a fictitious inertia tensor μ that effects a simple adjustment of the relative nuclear and electronic time scales. The *fictitious* dynamics thus obtained oscillates about the Born-Oppenheimer surface with controllable deviations^{74,76} and agrees well with Born-Oppenheimer dynamics calculations.^{75,79} ADMP has also been shown to be computationally superior to Born-Oppenheimer dynamics^{75,78,79} on account of relaxation of the self-consistent field (SCF) convergence criterion in ADMP. Several interesting problems^{25,27,75,78,79} have been studied using ADMP; perhaps the most notable among these include (a) a recent demonstration²⁷ that dynamical effects are critical in obtaining good infrared spectroscopic properties of flexible systems in agreement with experiment and (b) the prediction of the “amphiphilic” nature of the hydrated proton^{25–27} in water clusters. Some well-documented advantages of ADMP^{71,74–76} include asymptotic linear scaling of computation time with system size, efficient use of reasonably larger time steps for propagation, ability to use accurate hybrid or gradient-corrected density functionals, and the ability to use chemically accurate basis sets. These critical features of ADMP allow the reliable study of reactive processes in systems with moderate (over 100) number of atoms.⁷⁸ In Refs. 80 and 81 ADMP and Born-Oppenheimer dynamical methods have been generalized in conjunction with quantum wave-packet dynamics to facilitate efficient quantum dynamics in medium-sized systems.

Since there is no SCF convergence in ADMP, explicit error analysis is required to ascertain the accuracy of the dynamics. We outline two mechanisms^{74,76} that have been used in the current study. The commutator of the single-particle electronic density matrix (\mathbf{P}) and the Fock matrix (\mathbf{F}) is non-negligible in ADMP and plays a central role. The nuclear gradients include additional terms that depend on this commutator.^{71,76} Furthermore, the accuracy and efficiency of ADMP dynamics (determined by closeness to the Born-Oppenheimer surface) is also governed by this commutator and it places rigorous bounds on the allowed values of the fictitious tensor through the relation⁷⁶

$$\|[\mathbf{F}, \mathbf{P}]\|_F \geq \frac{1}{\|[\mathbf{P}, d\mathbf{P}/dt]\|_F} \left| \text{Tr} \left[\frac{d\mathbf{P}}{dt} \mu^{1/2} \frac{d^2\mathbf{P}}{dt^2} \mu^{1/2} \right] \right|, \quad (1)$$

where $\|[\dots]\|_F$ is the Frobenius norm⁸⁵ of the commutator defined as $\|A\|_F = \sqrt{\sum_{i,j} A_{i,j}^2}$. Thus μ places a lower bound on the commutator and restricts the dynamics to be at least a certain distance from the Born-Oppenheimer surface. Secondly, the rate of change

$$\frac{d\mathcal{H}_{\text{fict}}}{dt} = \text{Tr} \left[\frac{d\mathbf{P}}{dt} \mu^{1/2} \frac{d^2\mathbf{P}}{dt^2} \mu^{1/2} \right] \quad (2)$$

is required to be *bounded and oscillatory*⁷⁴ and this again is determined by the choice of fictitious tensor.

Equations (1) and (2) represent^{74,76} the instantaneous deviation of ADMP trajectories from adiabatic behavior. Although the ADMP trajectory does not exactly remain on the Born-Oppenheimer surface (due to no SCF convergence), it is required that long time averages provide similar results as in Born-Oppenheimer molecular dynamics. This leads to the requirement that the quantity in Eq. (2) be an oscillatory function such that its average value is small. There is, however, also a second condition enforced by Eq. (2), and this is the requirement that the instantaneous value of the quantity in Eq. (2) should be *bounded* and less than some predefined threshold. *Both conditions* must be met in order to maintain adiabatic behavior. One must monitor the quantities in Eqs. (1) and (2) to ascertain that the ADMP dynamics is physically consistent.

III. RESULTS AND DISCUSSION

To study the structure, dynamics, vibrational, and excited-state properties of HO₂-water clusters, we have carried out a series of optimization, frequency, ADMP dynamics, and time-dependent density-functional theory (TD-DFT) calculations on clusters of various sizes. All calculations are performed using the B3LYP density functional, double-zeta polarized diffused Gaussian basis set, and the Gaussian series of electronic structure programs.⁸⁶

For the HO₂(H₂O)₂₀ cluster we have carried out ADMP calculations including all electrons in the system. The basis set choice for this methodology is critical due to the computationally intensive nature of the approach when long simulation times are desired. The choice here (double-zeta polarized diffused Gaussian basis set and B3LYP density functional) is based on a detailed study of a variety of basis functions and density functionals, such as B3LYP, BLYP, and

BPBE, for the water dimer system, with and without basis set superposition error.⁷⁹ A time step of 0.25 fs and valence fictitious mass of 180 a.u., along with a tensorial mass-weighting scheme,⁷⁴ were employed as in previous ADMP studies.^{25,74,75,78–80}

Our initial structure for the dynamics had the HO₂ molecule solvated inside the cluster. This starting geometry is the second most stable geometry found in Ref. 13. The most stable geometry found in Ref. 13 had the HO₂ molecule on the surface of the cluster. As noted in Sec. I, the difference in energy between these two structures was only ≈ 1.7 kcal/mol. Hence, it was instructive to check if there exists a downhill potential gradient at finite temperature that would assist in “ejecting” the HO₂ molecule to its more stable conformer. This approach is very similar to that used in recent studies^{25–27} involving the protonated species in water clusters where it was found that the proton does indeed get “ejected” to the surface over a period of a few picoseconds (1–2 ps). A similar result here would certainly indicate the kinetic stability of the HO₂ molecule on the surface of the cluster. Hence, we tested the surface affinity of the HO₂ molecule through an ADMP simulation of length approximately 4 ps. The simulation was conducted under *NVE* (constant energy) conditions. The temperature of the system (calculated assuming equipartition theorem) was approximately 160 K with a deviation of ± 30 K. No thermostats were used to maintain a fixed temperature. Using a thermostat, more stringent constraints on the fluctuations in temperature can be enforced. However, since we use the ADMP simulation data in the current study to analyze the stability of the HO₂ molecule inside the cluster *and* to obtain dynamical information through time-correlation functions, using thermostats is not preferred. Temperatures attained during the simulations are close to the upper tropospheric temperature in the polar regions (~ 200 K, Refs. 87 and 88) where interesting HO₂–water chemistry is said to occur.^{87,88}

It was found that over the period of the simulation, the hydroperoxyl radical remained inside the cluster. This is especially interesting in light of recent studies,¹³ where it has been noted that the HO₂ molecule has lower energy on the surface of the 20-water dodecahedral cluster. Based on single-point geometry optimization and frequency calculations on many different structures, Shi *et al.*¹³ found the “surface state” of the HO₂–water cluster to be more stable by 1.7 kcal/mol. The fact that our dynamical studies retain the HO₂ molecule in the interior implies that the barrier between the interior and exterior states is significantly important compared to kT at 160 ± 30 K, the conditions of our simulation. Hence, the molecule appears to be kinetically stabilized in the center of the cluster under conditions of atmospheric significance. Higher temperature calculations with longer simulation times will be considered as part of future investigations to further probe the stability of the HO₂ molecule on the interior and on the surface of the water cluster. However, the difference in energy between the interior and surface states is small enough that both states must contribute at atmospheric temperature. Shi *et al.*¹³ have reached a similar

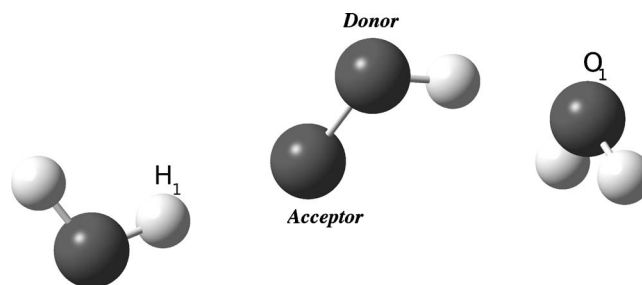


FIG. 1. Definitions for the structure descriptors used in Fig. 2. The dihedral angle is the angle between the planes formed by the O–O bond of HO₂ and the oxygen on the right, and the O–O bond of HO₂ and the oxygen on the left.

conclusion based on their study, and our results essentially complement their studies through the incorporation of dynamical effects.

The results found here differ from that found in protonated water clusters,^{25–27} where the protonated species spontaneously moves to the surface of the cluster. This result is, however, to be expected since the transport of the protonated species in water clusters occurs through the “Grotthuss” mechanism,²⁸ where the proton hops across an optimally placed chain of water molecules; the hopping process involves constant rearrangement of the bonding topology surrounding the hydrated proton. The transport of the HO₂ molecule as a whole, on the contrary, may be expected to be more diffusion limited.

Using the dynamics data we have, in addition, analyzed structural and spectroscopic properties of the cluster which are discussed in the following sections.

A. Structural properties

The structural distribution of configurations obtained during the ADMP simulation are shown in Fig. 2. The donor, acceptor, and dihedral angle are defined in Fig. 1. Figure 2(a) displays the distribution of distances between the acceptor oxygen and all other oxygen atoms in the system. Similarly, Fig. 2(b) represents the distribution of distances between the donor oxygen and other oxygens in the system. Figure 2(c) shows the distribution of dihedrals. An important feature is seen in Fig. 2(b) at about 2.5-Å O_{donor}–O distance. This distance is very similar to the O–O distance found in the protonated Zundel species, H₅O₂⁺, in water clusters.^{30,31,60,89} But here it corresponds to the distance between the donor oxygen and oxygen O₁ in Fig. 1. Another important feature is seen in Fig. 2(a) and corresponds to an O_{acceptor}–H₁ distance of approximately 1.9 Å. The strong peaks seen to the left in both Figs. 2(a) and 2(b) correspond to the bonded atomic distances. The dashed peak in Fig. 2(b) at ~ 3 Å represents the distance between the donor oxygen and neighboring non-bonded hydrogen atoms along with dynamical fluctuations. The broad feature seen in Figs. 2(a) and 2(b) around 4 Å is due to the additional solvation shells present in this system.

The Zundel-type peak found at 2.5 Å in Fig. 2(b) is intriguing. Generally, for a water dimer, the average distance

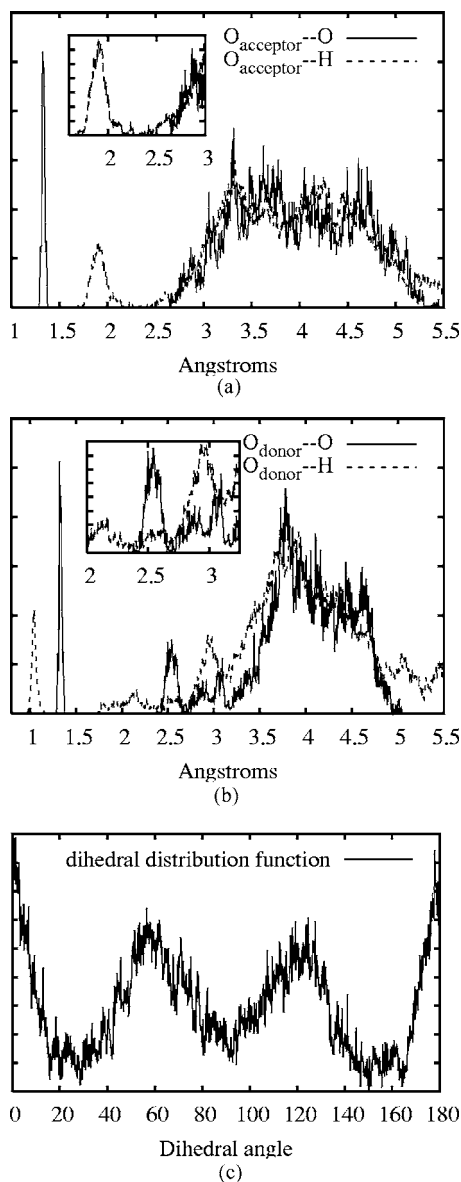


FIG. 2. Structural distribution obtained for the $\text{HO}_2(\text{H}_2\text{O})_{20}$ cluster found during ADMP dynamics. The temperature fluctuations during the dynamics are in the range 160 ± 30 K.

between neighboring oxygen atoms is about 2.9 Å. In the case of H_5O_2^+ the intervening excess proton allows the two oxygen atoms to get close to each other and a distance of about 2.45 Å is probable and this is close to where the peak is found in Fig. 2(b). By contrast, the Eigen cation, H_9O_4^+ (also commonly seen in protonated water clusters), has a most probable O–O distance of ~ 2.7 Å, since the positive charge is more delocalized in Eigen as compared to the Zundel ion. For the case of the HO_2 -water cluster studied here, there is no excess proton and, hence, the closer distance between the oxygen atoms initially comes as a surprise. However, upon closer inspection of the average partial charges seen during the dynamics, we note that the shared proton is electropositive as compared to the other water molecule hydrogens in the system which makes it acidic. The hydroperoxyl radical is known to be a weak acid⁵⁹ and this seems responsible for the shorter, Zundel-type, oxygen-oxygen distance noted here.

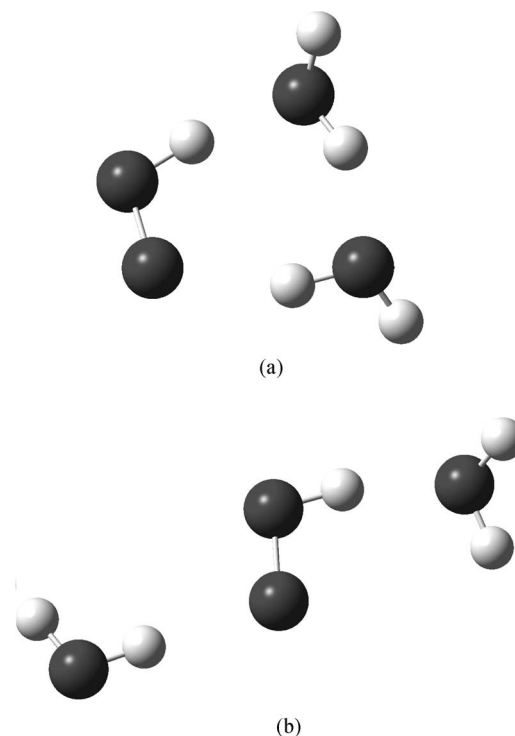


FIG. 3. $\text{HO}_2(\text{H}_2\text{O})_2$ structures: The structure in Fig. 3(a) is more stable by 8.2 kcal/mol.

To further investigate this interesting structural feature we conducted a potential-energy search for stable configurations in smaller clusters using the same level of density-functional theory (DFT) and basis set. We considered a single HO_2 molecule with two and three water molecules and the resulting stable structures are shown in Figs. 3 and 4. For the $\text{HO}_2(\text{H}_2\text{O})_2$ case, the structure with both waters on the same side [conformation in Fig. 3(a)] is more stable by about 8.2 kcal/mol. Part of this can be explained by the additional hydrogen bond present in the stable structure. The four structures in Fig. 4 are related: structures in Figs. 4(a) and 4(b) are related by one single concerted (cyclic) proton hop and this is also the case for structures in Figs. 4(c) and 4(d). However, the structure in Fig. 4(a) is most stable. On comparing the four structures obtained we note that as the number of water molecules is increased there is a definite propensity for the donor oxygen of HO_2 to get closer to the oxygen in the neighboring water molecule. The average $\text{O}_{\text{donor}}\text{--O}$ distance in $\text{HO}_2(\text{H}_2\text{O})_2$ is about 2.65 Å (which is consistent with previous studies²⁰ where a strong hydrogen-bonding character was detected in HO_2 water clusters), while this distance drops down to about 2.58 Å for the $\text{HO}_2(\text{H}_2\text{O})_3$ structures. The trend is consistent with the radial distributions we find for the $\text{HO}_2(\text{H}_2\text{O})_{20}$ case above.

Our results seem to indicate that as the number of water molecules is increased the polarizability of the water and HO_2 greatly influences the average structure of the cluster. The electronic distribution and subsequent polarizability of HO_2 and water are the reasons for the closer (Zundel-type) HO_2 -water distance. In Fig. 2 we also present the radial distribution function for the dihedral angle defined in Fig. 1.

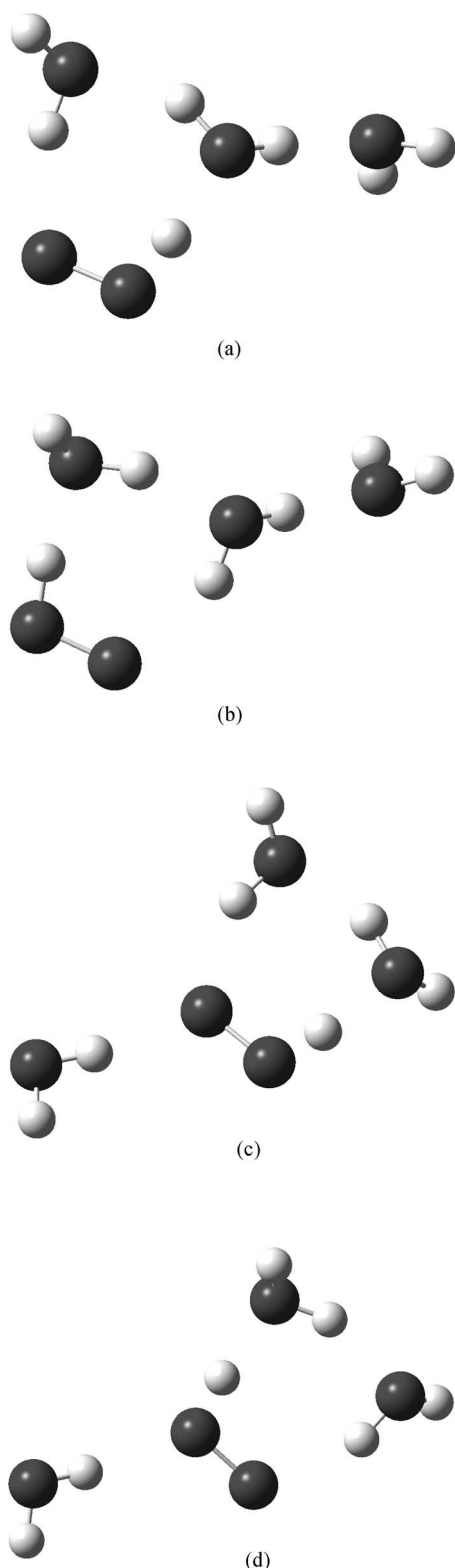


FIG. 4. $\text{HO}_2(\text{H}_2\text{O})_3$ structures: The structure in Fig. 4(a) is most stable. The structures in Figs. 4(a) and 4(b) are related by one single concerted (cyclic) proton hop. This is also the case for the structures in Figs. 4(c) and 4(d).

The peaks at 60° , 120° , and 180° are to be expected based on tetrahedral symmetry. However, there is substantial broadening of these peaks, implying fluctuations from the symmetric arrangement as a result of finite temperature effects during the dynamics process.

B. Vibrational properties

In Fig. 5(a) we display the behavior of the Fourier transform of the velocity autocorrelation function (FT-VAC) and Fourier transform of the dipole autocorrelation function (FT-DAC) obtained from ADMP. We also present in Fig. 5(a) the harmonic frequencies obtained from a single-point optimization (represented as Static/Freq. in Fig. 5) performed on one of the stable geometries obtained during the dynamics calculation. The FT-VAC represents the rovibrational density of states, while the FT-DAC is proportional to the experimentally measured IR intensities. It is important to note the difference between the FT-VAC and FT-DAC. The rovibrational density of states displayed in Fig. 5(a) interact with external radiation only if these exhibit a change in dipole moment during the corresponding motion. Consequently, the FT-DAC in Fig. 5(a), which indeed shows states accompanied by changing dipole moment has different intensities compared to the FT-VAC. The amplitudes for the FT-VAC may be related to amplitudes obtained from deep inelastic neutron-scattering studies of the vibrational properties.

The comparison between the FT-DAC and Static/Freq. spectra in Fig. 5(a) is interesting. While the bending ($\sim 1700\text{ cm}^{-1}$) and librational ($\sim 400\text{--}1000\text{ cm}^{-1}$) are in agreement between the spectra, the peaks at c.a. 2320, 2815, and around 3000 cm^{-1} (marked as “X” in Static/Freq. panel of Fig. 5) are almost completely missing in the spectra obtained from ADMP dynamics. These peaks in the harmonic frequencies involve a stretching mode of the oxygen-hydrogen bond belonging to HO_2 . Instead of these peaks the ADMP dynamics displays two extremely small peaks at around 2500 and 2800 cm^{-1} . This disagreement is rather interesting and upon closer inspection of the dynamics, we notice that this is precisely the portion of the system where the bonding topology changes most during the dynamics process. The shared proton performs many oscillations between the donor oxygen and the neighboring water and these vibrations are facilitated by the dynamics of the rest of the water cluster. As the proton performs the back-and-forth hops, it samples different regions of potential-energy surface, displaying a changing infrared signature. Furthermore, the autocorrelation functions are a dynamical property that can be thought of as being obtained as a statistical average of many different configurations. Thus, the resultant spectrum is dynamically averaged and results in the lower intensity of the peaks in the intermediate region of the spectrum. Due to the change in the vibrational intensities in the $2000\text{--}3000\text{ cm}^{-1}$ region during dynamics (due to anisotropic change in the environment of the protonated species), the statistical average broadens and flattens this region out, thus reducing the intensity of the associated peaks. Of course, conformational sensitivity of IR spectra is not a new concept⁹⁰ and has been known in conformational analysis⁹¹ for a long time. Similar dynamical averaging has also been found²⁷ to enhance the agreement between experimental and theoretical infrared spectra in a recent study of protonated water clusters using ADMP.

In Figs. 5(b) and 5(c) we account for quantum nuclear

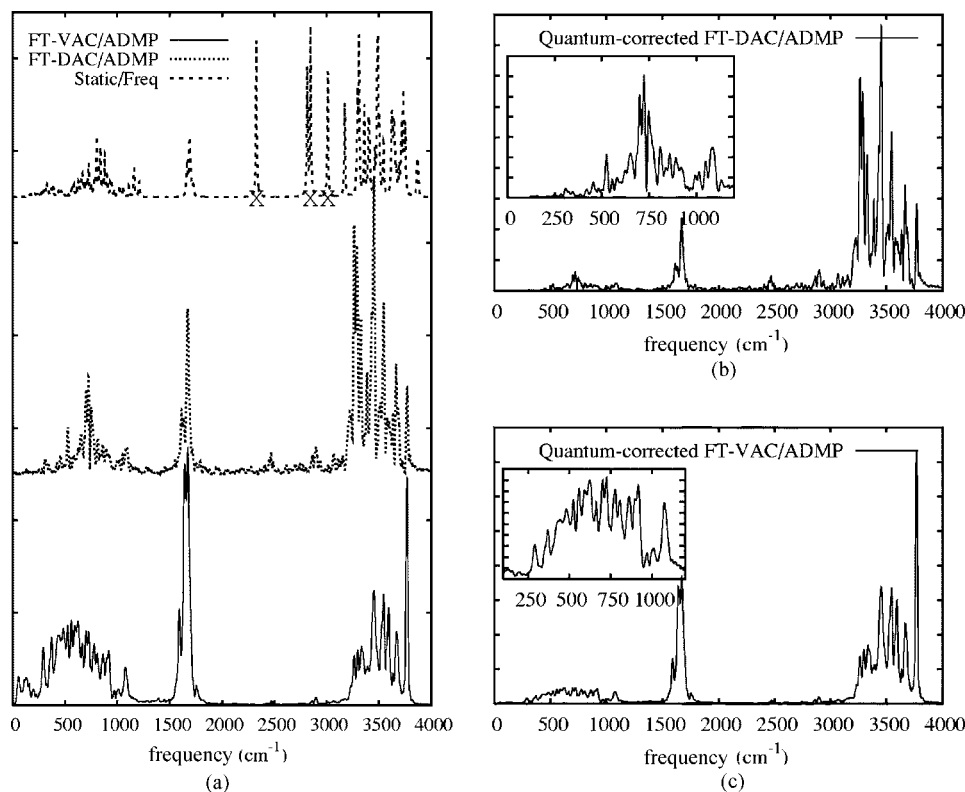


FIG. 5. In (a) we present harmonic frequencies for an optimized geometry (Static/Freq: dashed line) obtained from one of the structures sampled during ADMP dynamics, the vibrational density states obtained from the Fourier transform of the velocity autocorrelation function obtained from ADMP dynamics data (FT-VAC/ADMP: solid line) and the dipole autocorrelation function (FT-DAF/ADMP: dotted line). The strong peaks seen in the static case in the 2000–3000- cm^{-1} region (marked “X”) are completely nonexistent but for little peaks in the two bottom panels. This is due to dynamical averaging. See text for details. The dangling OH stretch is very clearly seen at c.a. 3770 cm^{-1} in all three spectra. [No scaling of frequencies has been employed (Ref. 22).] In (b) and (c) we present the Fourier transforms of the dipole and velocity autocorrelation functions but by including quantum nuclear corrections, within the harmonic approximation (Refs. 82–84) as in Eq. (3).

effects within the harmonic approximation.^{82–84} Here the classical correlation functions shown in Fig. 5(a) are corrected according to^{82–84}

$$C(\omega) \times \frac{\beta \hbar \omega}{1 - \exp[-\beta \hbar \omega]}, \quad (3)$$

where $C(\omega)$ is the classical correlation function and ω is the frequency in wave numbers. The correction factor is determined^{82,83} by assuming a harmonic oscillator potential for nuclear quantum effects. Our results indicate that the quantum effects within the harmonic approximation increase the intensities of the stretching modes. This is to be expected based on the prefactor in Eq. (3). Future studies will include full quantum dynamical effects for the HO_2 proton using a novel quantum wave-packet implementation of ADMP and Born-Oppenheimer dynamics.^{80,81}

C. Decay of HOMO-LUMO gap with cluster size

To study the reactive nature of the HO_2 system in the presence of water molecules, which can have important implications to atmospheric chemistry, we have looked at the distribution of electronic states and excitation energies by including dynamical effects. In Fig. 6(a) we present the distribution of electronic energies obtained from conformations sampled during the ADMP dynamics. Only states close to the Fermi level are shown for clarity. This figure shows the DFT

orbital energies for many different structures sampled during the dynamics process. The lowest unoccupied molecular orbital (LUMO) is indicated in the figure. Based on this we obtain the average highest occupied molecular orbital-lowest unoccupied molecular orbital (HOMO-LUMO) gap to be around 3.82 eV. It is further noted that the LUMO is isolated, as is to be expected from the fact that the system is a free radical. Consequently, an excess electron can be trapped into this low-lying LUMO, facilitating reactive processes or solvated electron chemistry. As a result, the HOMO-LUMO gap in this system is of interest and this aspect is discussed in further detail below.

To further investigate the effect of water on the HOMO-LUMO gap of the HO_2 radical, we have studied the dependence of the gap with increasing number of water molecules in the system. This dependence is shown in Table I for a few smaller clusters along with the 20-water cluster. For the smaller clusters, the gap is obtained at optimized geometries. For the two- and three-water cluster multiple minima were considered (see Figs. 3 and 4) and the values noted in Table I are obtained from a Boltzman average. The striking feature seen in this table is the monotonic decrease in the HOMO-LUMO gap with increasing number of water molecules. There is a 0.4-eV (≈ 9.6 kcal/mol) reduction in gap as one moves from 0 to 20 water molecules. The lower values are now close to those seen in wide band-gap semiconductors. Similarly, significant redshifts in the vertical excited-state en-

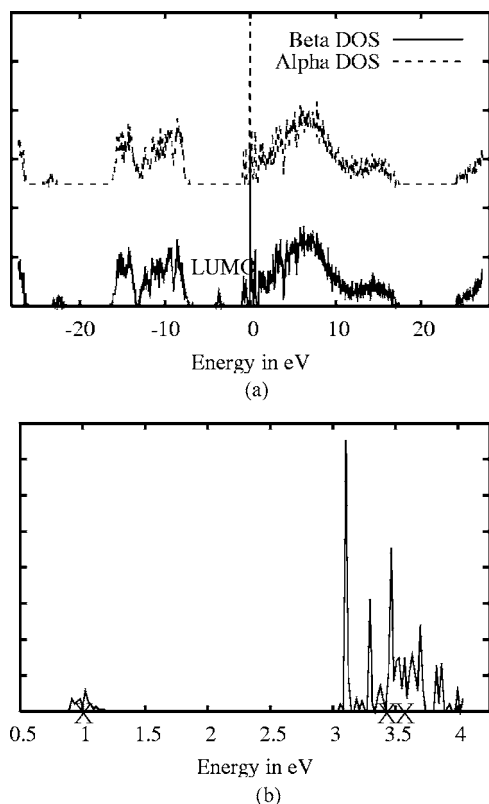


FIG. 6. (a) Unrestricted spin density of states for the α and β electrons obtained during ADMP dynamics. The α electronic states have been shifted for clarity. The average HOMO-LUMO gap is listed in Table I. The LUMO density of states is marked. (b) Vibrational broadening of TD-DFT excitations. The broadening is based on populations obtained from ADMP dynamics. The average values of the three excitation energies displayed are marked on the abscissa. As can be seen from the distribution of the larger excitations, the average geometry is not truly indicative of the fluctuations in the excitation energies obtained from dynamics.

ergies of the $\text{HO}_2\text{-H}_2\text{O}$ complex with respect to a single HO_2 molecule have been previously noted.¹⁹ Our results essentially complement these results. This is particularly interesting since water clusters are abundant in the upper troposphere and medium-sized water clusters have been used as models for cloud droplets.¹³ Furthermore, in the upper troposphere the concentration^{87,88} of $[\text{HO}_2]$ is 6×10^7 molecules/ cm^3 , that of $[\text{H}_2\text{O}]$ is 3×10^{13} molecules/ cm^3 and the total air concentration is approximately 5×10^{18} molecules/ cm^3 . If the HOMO-LUMO gap of HO_2 were reduced due to its interactions with water clusters, this would imply a greater probability of participation of the excited electronic states in the chemical reactions involving “sol-

TABLE I. HOMO-LUMO gaps (in eV).

Number of water molecules	HOMO-LUMO gap
0	4.2398
1	4.1750
2 ^a	4.0997
3	4.0643
20 ^b	3.8216 ± 0.1^c

^aTwo local minima. See text for details.

^bObtained from ADMP dynamical averaging. See Fig. 6(a).

^cThe distribution of gaps obtained from the dynamics run.

vated” HO_2 . This could have important consequences in atmospheric solvated electron chemistry and the reaction of solvated HO_2 with metal ions such as Fe^{2+} and Cu^+ , which are commonly found in aerosols.¹⁴

D. Dynamical broadening of excitation spectrum

To further investigate the excitation properties of the $\text{HO}_2(\text{H}_2\text{O})_{20}$ cluster, we have carried out TD-DFT calculations on a set of configurations obtained during the ADMP dynamics. This calculation not only provides us with the excitation energies, but it also provides us with additional information as to how these excitations change due to the change in nuclear geometry. Our results are shown in Fig. 6(b), where we plot the average excitation frequencies against dynamically averaged (cumulative) oscillator strengths obtained from 40 different conformations spread evenly over the length of the dynamics trajectory (of ≈ 4 ps). As can be seen the average value of the major excitation is in fairly good agreement with the HOMO-LUMO gap. (The excitation at about 1 eV shows a very low intensity since the oscillator strength of this excitation is zero for most conformations obtained during the dynamics.) However, there is substantial dynamical broadening, which indicates that different portions of the potential-energy surface are sampled during the process and, hence, temperature and dynamical sampling play a critical role on excited-state behavior of HO_2 -water clusters. Furthermore, in the current simulation the nature of this broadening is not only due to Doppler effect, but also due to the changing electron density and bonding topology encountered during the *ab initio*-based ADMP approach. This effect is very similar to what we see in Sec. III B for the vibrational spectra. Similar dynamical broadening has been found in other solute-solvent systems;⁹² in our case this effect is seen as a result of the dynamical bonding topology of the HO_2 -water system. Precise broadening line shapes will require longer dynamics trajectories and extensive sampling, which will be part of future investigations.

It is also interesting to note that once the dynamical broadening is included in the flexible water cluster system, the agreement between the HOMO-LUMO gap and the excitation spectrum is quite reasonable. This is a surprising result since it is known that Kohn-Sham orbital energies are generally *not* a good approximation to excitation spectrum and ionization potentials. The results here are, of course, still within the Born-Oppenheimer approximation and including nonadiabatic effects and quantum nuclear effects can further affect this broadening. However, it is already clear that using a single geometry to predict the excitation spectrum for flexible systems such as those considered here is not reliable. This result is consistent with similar observations found for the vibrational properties of protonated systems.²⁷ Our trajectories, however, are still relatively short. While it cannot be ruled out that further structural relaxation is possible over a longer simulation, the stability of our system, over the period of simulation suggests that the system has settled into a (possibly) metastable state. Further analysis of the spread of the excitation spectrum with reference to simulation

length and multiple starting geometries will be the subject of future publications.

IV. CONCLUSIONS

We have performed *ab initio* single-point optimization, frequency, ADMP dynamics, and TD-DFT calculations on HO₂-water clusters of various sizes. There are three significant results that we have obtained as part of this study. Firstly, we find that the HO₂-water system displays an isolated, low-lying LUMO on account of being a free radical. Furthermore, the dynamically averaged HOMO-LUMO gap monotonically decreases as the number of water molecules is increased in an HO₂-water cluster. For the 20 water-cluster system studied here the gap is already in the wide band-gap semiconductor region. This aspect is interesting because a low-lying isolated LUMO presents a trap for an excess electron to promote solvated electron chemistry. In aqueous aerosol chemistry, it is well known^{14,59} that HO₂ solvated in water clusters reacts with divalent cations such as Fe²⁺ and monovalent cations such as Cu⁺ and this comprises an important HO₂ sink in the troposphere. Such reactions could be assisted by the lower HOMO-LUMO gap and isolated low-lying LUMO in solvated HO₂.

Another important conclusion that arises from our study is that the dynamical averaging of the potential-energy surface greatly affects the excitation as well as the infrared spectra of such flexible water cluster systems. We find that the dynamics could *spread* the excitation energy spectrum by as much as 1 eV at temperatures that are significant in the earth's atmosphere. Once dynamical averaging is taken into account, the agreement between the HOMO-LUMO gap and electronic excitation energy is surprisingly good. This further illustrates that single-point excitation spectrum calculations on flexible systems will not, in general, lead to reliable results. We also find similar effects for vibrational properties; dynamical effects can give rise to marked deviations from the corresponding harmonic spectra especially for flexible systems like those treated here. These effects could be further compounded due to nuclear quantum effects and this has been indicated by previous gas-phase quantum dynamics studies.⁹³⁻⁹⁶ Thus, future studies will include quantum dynamical treatment of the "hopping" proton in HO₂, while treating the rest of the nuclei classically along with accurate treatment of the electrons within ADMP, as allowed by a novel quantum dynamics formalism.^{80,81} This will help understand the extent to which quantum dynamics plays a role in HO₂ water clusters.

Finally, from a structural analysis of our dynamics trajectory simulation, we find that the HO₂ molecule is solvated primarily by two neighboring water molecules. Interestingly, the distance between the donor oxygen of HO₂ and its neighboring water molecule is similar to that found in the Zundel H₅O₂⁺ ion from protonated water clusters. The reason for this is due to the fact that on average the proton in HO₂ is acidic, which we obtain from a charge analysis of our dynamics trajectory. Furthermore, due to the inherent symmetry of the solvated system shown in Fig. 1, we believe that the zwitterionic form of this species will remain probable in larger

water clusters if the HO₂ molecule has a significant probability of remaining solvated inside the water cluster.

ACKNOWLEDGMENTS

This research was supported by the Camille and Henry Dreyfus New Faculty Award Program and the Indiana University, Chemistry Department. The author (S.S.I.) is a Camille and Henry Dreyfus New Faculty awardee. Important discussions on the topic with Professor Philip S. Stevens and Professor Joseph S. Francisco are duly acknowledged.

- ¹S. Solomon, R. R. Garcia, F. S. Rowland, and D. J. Wuebbles, *Nature (London)* **321**, 755 (1986).
- ²B. J. Finlayson-Pitts and J. N. Pitts, Jr., *Chemistry of the Upper and Lower Atmosphere: Theory, Experiments, and Applications* (Academic, San Diego, 2000).
- ³R. P. Turco, O. B. Toon, and P. Hamil, *J. Geophys. Res.* **94**, 16493 (1989).
- ⁴S. Solomon, *Rev. Geophys.* **37**, 275 (1999).
- ⁵D. E. Heard and M. J. Pilling, *Chem. Rev. (Washington, D.C.)* **103**, 5163 (2003).
- ⁶J. Troe, *Proc. Combust. Inst.* **28**, 1463 (2000).
- ⁷J. A. Logan, M. J. Prather, S. C. Wofsy, and M. B. McElroy, *J. Geophys. Res.* **86**, 7210 (1981).
- ⁸M. J. McEwan and L. F. Phillips, *Acc. Chem. Res.* **3**, 9 (1970).
- ⁹A. W. Castleman and R. G. Keese, *Chem. Rev. (Washington, D.C.)* **86**, 589 (1986).
- ¹⁰M. J. McEwan and L. F. Phillips, *Chemistry of the Atmosphere* (Edward Arnold, London, 1975).
- ¹¹R. P. Wayne, *Chemistry of the Atmosphere* (Clarendon, Oxford, 1994).
- ¹²J. S. Aloisio and S. Francisco, *Acc. Chem. Res.* **33**, 825 (2000).
- ¹³Q. Shi, S. D. Belair, J. S. Francisco, and S. Kais, *Proc. Natl. Acad. Sci. U.S.A.* **100**, 9686 (2003).
- ¹⁴J. Thornton and J. P. D. Abbat, *J. Geophys. Res.* **110**, D08309 (2005).
- ¹⁵B. J. Gertner and J. T. Hynes, *Science* **271**, 1563 (1996).
- ¹⁶J. P. Devlin, N. Uras, J. Sadlej, and V. Buch, *Nature (London)* **417**, 269 (2002).
- ¹⁷D. R. Hanson, A. R. Ravishankara, and S. Solomon, *J. Geophys. Res., [Atmos.]* **99**, 3615 (1994).
- ¹⁸S. D. Belair, H. Hernandez, and J. S. Francisco, *J. Am. Chem. Soc.* **126**, 3024 (2004).
- ¹⁹S. Aloisio, Y. Li, and J. S. Francisco, *J. Chem. Phys.* **110**, 9017 (1999).
- ²⁰S. Aloisio and J. S. Francisco, *J. Phys. Chem. A* **102**, 1899 (1998).
- ²¹R. Vacha, P. Slavicek, M. Mucha, B. Finlayson-Pitts, and P. Jungwirth, *J. Phys. Chem. A* **108**, 11573 (2004).
- ²²J.-W. Shin, N. I. Hammer, E. G. Diken *et al.*, *Science* **304**, 1137 (2004).
- ²³T. S. Zwier, *Science* **304**, 1119 (2004).
- ²⁴M. Miyazaki, A. Fujii, T. Ebata, and N. Mikami, *Science* **304**, 1134 (2004).
- ²⁵S. S. Iyengar, T. J. F. Day, and G. A. Voth, *Int. J. Mass. Spectrom.* **241**, 197 (2005).
- ²⁶M. K. Petersen, S. S. Iyengar, T. J. F. Day, and G. A. Voth, *J. Phys. Chem. B* **108**, 14804 (2004).
- ²⁷S. S. Iyengar, M. K. Petersen, T. J. F. Day, C. J. Burnham, V. E. Teige, and G. A. Voth, *J. Chem. Phys.* **123**, 084309 (2005).
- ²⁸N. Agmon, *Chem. Phys. Lett.* **244**, 456 (1995).
- ²⁹S. Wei, Z. Shi, and A. W. Castleman, Jr., *J. Chem. Phys.* **94**, 3268 (1991).
- ³⁰M. Eigen and L. D. Maeyer, *Proc. R. Soc. London, Ser. A* **247**, 505 (1958).
- ³¹G. Zundel, in *The Hydrogen Bond-Recent Developments in Theory and Experiments*, II. Structure and Spectroscopy (North-Holland, Amsterdam, 1976), pp. 683-766.
- ³²R. P. Bell, *The Proton in Chemistry* (Cornell University Press, Ithaca, NY, 1973).
- ³³R. M. Lynden-Bell and J. C. Rasaiah, *J. Chem. Phys.* **105**, 9266 (1996).
- ³⁴R. Pomes and B. Roux, *Biophys. J.* **71**, 19 (1996).
- ³⁵H. Decornez, K. Drukker, and S. Hammes-Schiffer, *J. Phys. Chem. A* **103**, 2891 (1999).
- ³⁶M. L. Brewer, U. W. Schmitt, and G. A. Voth, *Biophys. J.* **80**, 1691 (2001).
- ³⁷C. J. Tsai and K. D. Jordan, *Chem. Phys. Lett.* **213**, 181 (1993).

- ³⁸S. S. Xantheas, J. Chem. Phys. **102**, 4505 (1995).
- ³⁹S. Sadhukhan, D. Munoz, C. Adamo, and G. E. Scuseria, Chem. Phys. Lett. **306**, 83 (1999).
- ⁴⁰Y. Xie, R. B. Remington, and H. F. Schaefer III, J. Chem. Phys. **101**, 4878 (1994).
- ⁴¹S. J. Singer, S. McDonald, and L. Ojamae, J. Chem. Phys. **112**, 710 (2000).
- ⁴²R. R. Sadeghi and H.-P. Cheng, J. Chem. Phys. **111**, 2086 (1999).
- ⁴³D. Wei and D. R. Salahub, J. Chem. Phys. **106**, 6086 (1997).
- ⁴⁴M. E. Tuckerman, K. Laasonen, M. Sprik, and M. Parrinello, J. Phys. Chem. **99**, 5749 (1995).
- ⁴⁵D. Marx, M. E. Tuckerman, J. Hutter, and M. Parrinello, Nature (London) **397**, 601 (1999).
- ⁴⁶A. Banerjee, A. Quigley, R. F. Frey, D. Johnson, and J. Simons, J. Am. Chem. Soc. **109**, 1038 (1987).
- ⁴⁷X.-D. Xiao, V. Vogel, and Y. R. Shen, Chem. Phys. Lett. **163**, 555 (1989).
- ⁴⁸C. Rädüge, V. Pflumio, and Y. R. Shen, Chem. Phys. Lett. **274**, 140 (1997).
- ⁴⁹M. Okumura, L. I. Yeh, J. D. Myers, and Y. T. Lee, J. Phys. Chem. **94**, 3416 (1990).
- ⁵⁰T. F. Magnera, D. E. David, and J. Michl, Chem. Phys. Lett. **182**, 363 (1991).
- ⁵¹D. Asthagiri, L. R. Pratt, J. D. Kress, and M. A. Gomez, Proc. Natl. Acad. Sci. U.S.A. **101**, 7229 (2004).
- ⁵²M. E. Tuckerman, D. Marx, and M. Parrinello, Nature (London) **417**, 925 (2002).
- ⁵³N. Agmon, Chem. Phys. Lett. **319**, 247 (2000).
- ⁵⁴L. Perera and M. L. Berkowitz, J. Chem. Phys. **95**, 1954 (1991).
- ⁵⁵L. Perera and M. L. Berkowitz, J. Chem. Phys. **96**, 8288 (1992).
- ⁵⁶E. M. Knipping, M. J. Lakin, K. L. Foster, P. Jungwirth, D. J. Tobias, R. B. Gerber, D. Dabdub, and B. J. Finlayson-Pitts, Science **288**, 301 (2000).
- ⁵⁷U. Achatz, B. S. Fox, M. K. Beyer, and V. E. Bondybey, J. Am. Chem. Soc. **123**, 6151 (2001).
- ⁵⁸E. D. Sloan, Jr., *Clathrate Hydrates of Natural Gases* (Marcel Dekker, New York, 1998).
- ⁵⁹D. J. Jacob, Atmos. Environ. **34**, 2131 (2000).
- ⁶⁰D. Eisenberg and W. Kauzman, *The Structure and Properties of Water* (Oxford University Press, Oxford, 1969).
- ⁶¹J. A. Miller, R. J. Kee, and C. K. Westbrook, Annu. Rev. Phys. Chem. **41**, 345 (1990).
- ⁶²R. V. Martin, D. J. Jacob, R. M. Yantosca, M. Chin, and P. Ginoux, J. Geophys. Res. **108**, 4097 (2003).
- ⁶³I. S. Y. Wang and M. Karplus, J. Am. Chem. Soc. **95**, 8160 (1973).
- ⁶⁴C. Leforestier, J. Chem. Phys. **68**, 4406 (1978).
- ⁶⁵R. Car and M. Parrinello, Phys. Rev. Lett. **55**, 2471 (1985).
- ⁶⁶D. Marx and J. Hutter, *Ab Initio Molecular Dynamics: Theory and Implementation* (John von Neumann Institute for Computing, Julich, 2000), Vol. 1, pp. 301-449.
- ⁶⁷H. B. Schlegel, J. Comput. Chem. **24**, 1514 (2003).
- ⁶⁸M. C. Payne, M. P. Teter, D. C. Allan, T. A. Arias, and J. D. Joannopoulos, Rev. Mod. Phys. **64**, 1045 (1992).
- ⁶⁹E. Deumens, A. Diz, R. Longo, and Y. Öhrn, Rev. Mod. Phys. **66**, 917 (1994).
- ⁷⁰K. Bolton, W. L. Hase, and G. H. Peslherbe, *Modern Methods for Multidimensional Dynamics Computation in Chemistry* (World Scientific, Singapore, 1998), p. 143.
- ⁷¹H. B. Schlegel, J. M. Millam, S. S. Iyengar, G. A. Voth, A. D. Daniels, G. E. Scuseria, and M. J. Frisch, J. Chem. Phys. **114**, 9758 (2001).
- ⁷²P. A. M. Dirac, *The Principles of Quantum Mechanics*, The International Series of Monographs on Physics Vol. 27, 4th ed. (Oxford University Press, New York, 1958).
- ⁷³J. Frenkel, *Wave Mechanics* (Oxford University Press, Oxford, 1934).
- ⁷⁴S. S. Iyengar, H. B. Schlegel, J. M. Millam, G. A. Voth, G. E. Scuseria, and M. J. Frisch, J. Chem. Phys. **115**, 10291 (2001).
- ⁷⁵H. B. Schlegel, S. S. Iyengar, X. Li, J. M. Millam, G. A. Voth, G. E. Scuseria, and M. J. Frisch, J. Chem. Phys. **117**, 8694 (2002).
- ⁷⁶S. S. Iyengar, H. B. Schlegel, G. A. Voth, J. M. Millam, G. E. Scuseria, and M. J. Frisch, Isr. J. Chem. **42**, 191 (2002).
- ⁷⁷S. S. Iyengar, H. B. Schlegel, and G. A. Voth, J. Phys. Chem. A **107**, 7269 (2003).
- ⁷⁸N. Rega, S. S. Iyengar, G. A. Voth, H. B. Schlegel, T. Vreven, and M. J. Frisch, J. Phys. Chem. B **108**, 4210 (2004).
- ⁷⁹S. S. Iyengar and M. J. Frisch, J. Chem. Phys. **121**, 5061 (2004).
- ⁸⁰S. S. Iyengar and J. Jakowski, J. Chem. Phys. **122**, 114105 (2005).
- ⁸¹S. S. Iyengar, Theor. Chem. Acc. (in press).
- ⁸²P. H. Berens, S. R. White, and K. R. Wilson, J. Chem. Phys. **75**, 515 (1981).
- ⁸³J. S. Bader and B. J. Berne, J. Chem. Phys. **100**, 8359 (1994).
- ⁸⁴C. P. Lawrence, A. Nakayama, N. Makri, and J. L. Skinner, J. Chem. Phys. **120**, 6621 (2004).
- ⁸⁵G. H. Golub and C. F. van Loan, *Matrix Computations* (Johns Hopkins University Press, Baltimore, 1996).
- ⁸⁶M. J. Frisch, G. W. Trucks, H. B. Schlegel *et al.*, GAUSSIAN 03, revision b.02 Gaussian, Inc., Pittsburgh, PA, 2003.
- ⁸⁷P. O. Wennberg, T. F. Hanisco, L. J. D. J. Jacob *et al.*, Science **279**, 49 (1998).
- ⁸⁸G. P. Brasseur, J. J. Orlando, and G. S. Tyndall, *Atmospheric Chemistry and Global Change* (Oxford University Press, New York, 1999).
- ⁸⁹M. Eigen, Angew. Chem., Int. Ed. Engl. **3**, 1 (1964).
- ⁹⁰F. J. Devlin and P. J. Stephens, J. Am. Chem. Soc. **121**, 7413 (1999).
- ⁹¹E. L. Eliel, N. Allinger, S. J. Angyal, and G. A. Morrison, *Conformational Analysis* (Wiley-Interscience, New York, 1965).
- ⁹²A. D. Stein and M. Fayer, Chem. Phys. Lett. **176**, 159 (1991).
- ⁹³R. T. Pack, E. A. Butcher, and G. A. Parker, J. Chem. Phys. **99**, 9310 (1993).
- ⁹⁴C. Leforestier and W. H. Miller, J. Chem. Phys. **100**, 733 (1994).
- ⁹⁵V. A. Mandelshtam, H. S. Taylor, and W. H. Miller, J. Chem. Phys. **105**, 496 (1996).
- ⁹⁶S. C. Althorpe and D. C. Clary, Annu. Rev. Phys. Chem. **54**, 493 (2003).